Chapter 34

Optical Coherence Tomography of the Oral Cavity and Pharynx: Normative Anatomy and Benign Processes

Giriraj K. Sharma and Brian J.-F. Wong

Introduction

At present, otolaryngologists have limited options for in vivo diagnosis of head and neck pathology. Workup of suspicious lesions of the OC or pharynx begins with a systematic office-based head and neck examination. With assistance of a headlamp or flashlight, the surgeon can quickly examine the OC to assess a patient's general health status and identify suspicious lesions. Visual assessment and digital palpation of the lips, buccal mucosa, gingiva, teeth, retromolar trigone, tongue, and floor of mouth are performed in a systematic manner to assess for textural and structural irregularities, color, and odor. Next, the tongue is relaxed or depressed with a tongue blade to visually examine the oropharynx (OP) for mucosal color, structural integrity, antero-posterior and lateral dimensions, tonsillar symmetry, and uvula movement and symmetry. Examination of the nasopharynx (NP), hypopharynx, and larynx requires an indirect mirror exam or can be performed by flexible fiber-optic nasopharyngoscopy. A significant limitation, however, to visual inspection, flexible, or rigid endoscopy is that these examinations only permit subjective evaluation of surface tissues. At present, surgeons lack a practical diagnostic modality which allows for in vivo high-resolution imaging of subepithelial tissue in the event of suspicious oral or pharyngeal lesions. Computed tomography (CT) and magnetic resonance (MR) imaging do not have adequate resolution to differentiate between benign and malignant lesions. Furthermore, both procedures may require sedation for pediatric patients and CT carries the risk of ionizing radiation. The only way to definitively differentiate between benign, premalignant, and malignant lesions is histopathological analysis of excised tissue. This is an invasive

Brian J.-F. Wong and Justus Ilgner (eds.), *Biomedical Optics in Otorhinolaryngology: Head and Neck Surgery*,
DOI 10.1007/978-1-4939-1758-7_34, © Springer Science+Business Media New York 2016

procedure, associated with patient morbidity, cost, poor coverage of at-risk tissue, and, in many cases, a delayed diagnosis of advanced-stage lesions.

A variety of inflammatory lesions and benign pathology may occur in the OC and pharynx. Tumors of the OC and OP are generally grouped together, with the OC being a more common site for benign pathology. These include inflammatory hyperplasias (e.g., fibroma, pyogenic or giant cell granuloma, and benign lymphoid hyperplasia), hamartomas (e.g., lymphangioma, hemangioma, neurofibroma, granular cell tumor, and lipoma), benign epithelial tumors (e.g., pleomorphic adenoma), benign tumors of the bone, benign odontogenic tumors, and cysts. Additional benign oral conditions include candidiasis, aphthous ulcers, recurrent herpes labialis, erythema migrans, lichen planus, and hyperkeratosis [1]. Dysplastic lesions include leukoplakia (white), erythroplakia (red), or mixed white-red epithelial lesions. Leukoplakias develop in 1–4 % of the population, with a reported 0.13–33 % of these lesions undergoing malignant transformation [2, 3]. Erythroplakias carry risk for malignant conversion in up to 85 % of lesions [3]. Benign tumors of the NP are rare and occur more commonly in children and young adults. These include developmental tumors (e.g., teratomas), ectodermal tumors (e.g., papillomas and adenomatous polyps), mesodermal tumors (e.g., juvenile angiofibroma, fibromyxomatous polyps, osteomas, and fibrous dysplasia), and benign salivary gland tumors [4]. Tumors of the NP have a capacity for undetected growth and expansion, often leading to a delay in the onset of symptoms which, combined with the diagnostic inaccessibility of the NP, often results in delayed diagnosis.

Anatomy

The OC has several functions including the sense of taste, mastication, and deglutition and is involved in vocalization and respiration. The OC is bounded anteriorly at the vermilion border of the lip, laterally by the cheeks and tonsillar pillars, and extends posteriorly to the hard–soft palate junction (superior boundary) and circumvallate papillae (inferior boundary). Oral mucosa consists of stratified squamous epithelium and underlying connective tissue (lamina propria) which are separated by a basal lamina. The lamina propria is divided into a papillary layer (superficial) and a more fibrous layer (deep). Classifications of oral mucosa are based upon location and function, including masticatory mucosa (keratinized stratified squamous epithelium), lining mucosa (non-keratinized stratified squamous epithelium), and specialized mucosa in the regions of the taste buds. OCT images of normal buccal mucosa (non-keratinized stratified squamous epithelium) are depicted in Fig. 1. In contrast,

the lips contain keratinized epithelium, as noted by a distinct contrast difference in the epithelial layer in Fig. 2. Figure 3 depicts OCT images of the normal floor of the mouth.

The pharynx participates in vocalization, digestive, and respiratory functions and is divided into three anatomical sections: the NP, OP, and laryngopharynx. The NP is bounded anteriorly by the choanae, superiorly by the body of the sphenoid bone (base of skull), laterally by the Eustachian tube orifices, and posteriorly by the superior constrictor muscles. Nasopharyngeal soft tissue is composed of various epithelial (keratinized and non-keratinized squamous, pseudostratified, ciliated, and columnar), glandular, and lymphoid tissues. The OP is posterior to the OC and is bounded by the soft palate superiorly and hyoid bone inferiorly. Posterior and lateral boundaries are formed by the muscular pharyngeal wall (superior and middle constrictors). The laryngopharynx or hypopharynx is

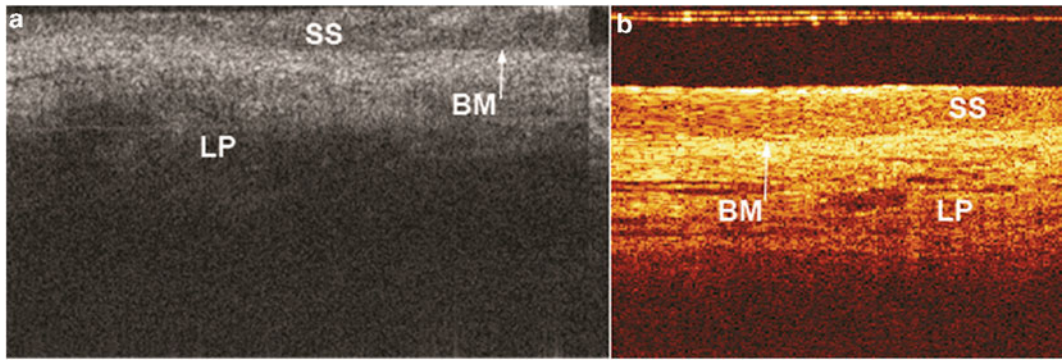

Fig. 1 OCT images of normal buccal mucosa acquired from a university-built TD-OCT system (**a**) and a commercially available system (**b**). *SS* non-keratinized stratified squamous epithelium, *BM* basement membrane, *LP* lamina propria

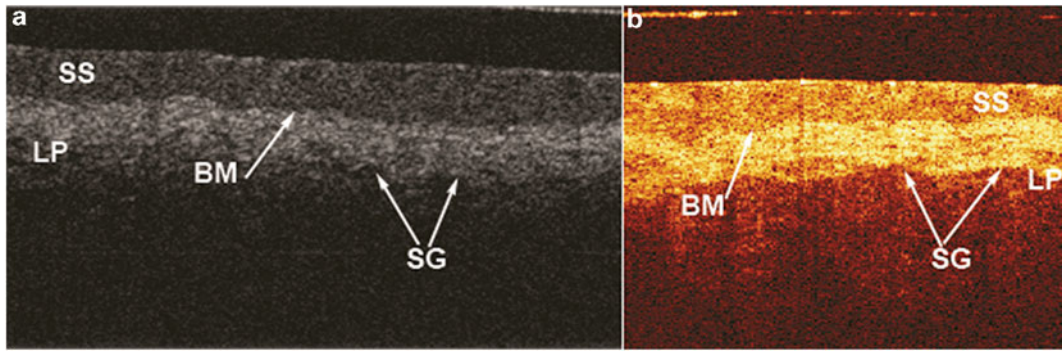

Fig. 2 OCT images of normal lip mucosa acquired from a research TD-OCT system (**a**) and a commercially available system (**b**). *SS* keratinized stratified squamous epithelium, *BM* basement membrane, *LP* lamina propria, *SG* seromucinous glands

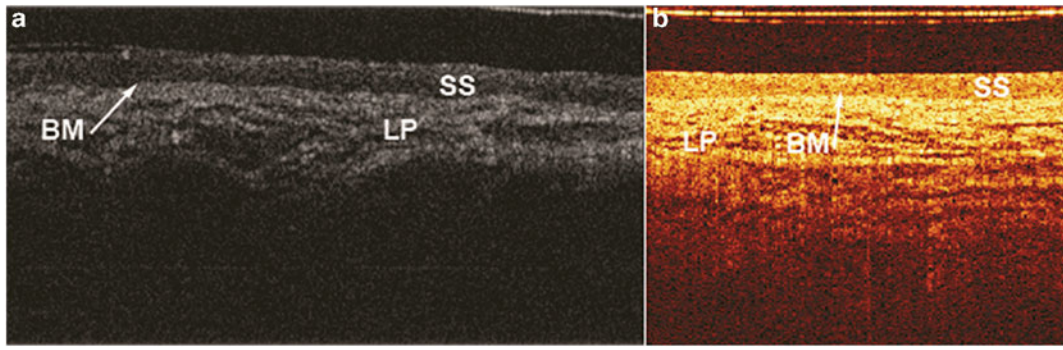

Fig. 3 OCT images of normal floor of mouth acquired from a research TD-OCT system (**a**) and a commercially available system (**b**). *SS* keratinized stratified squamous epithelium, *BM* basement membrane, *LP* lamina propria

the caudal most section of the pharynx and lies inferior to the epiglottis and is bounded laterally by the aryepiglottic folds. The laryngopharynx communicates inferiorly with the esophagus (posteriorly) and larynx (anteriorly). The OP and laryngopharynx are lined by non-keratinized stratified squamous epithelium.

Principles of OCT

In the last 10 years, substantial research in optical diagnostics has increased our understanding of the relationship between the optical and biologic properties of tissues. By detecting alterations in light–tissue interaction, optical technologies can provide real-time assessment of tissue structure and physiologic state at a molecular level. Furthermore, optical diagnostics have the potential to identify early precancerous changes which are frequently undetectable by visual examination. Current noninvasive or minimally invasive optical technologies include photosensitizers, in vivo confocal and multiphoton imaging microscopy, spectroscopy (e.g., Raman spectroscopy, elastic scattering spectroscopy, and fluorescence spectroscopy), and OCT. While the benefits of optical diagnostics vary with each technology, common advantages over histopathological examination include a real-time diagnosis, decreased morbidity, and cost. Furthermore, certain optical imaging modalities (e.g., spectroscopy) offer objective data analysis which may reduce diagnostic subjectivity commonly associated with the interpretation of tissue samples.

OCT is a light-based imaging modality which is based upon principles of low coherence interferometry [5, 6]. A near-infrared light source (e.g., laser or superbright light emitting diode) is split into two paths culminating in a mirror (reference arm) and biological

tissue (sample arm), respectively. Back-reflected light from the reference and sample arms is recombined and detected to construct interference profiles (A-lines) as a function of tissue depth. Individual and adjacent A-lines are combined to form a three-dimensional (3D), cross-sectional images of tissue. OCT is able to provide real-time images with resolution up to 10–15 μm and optical penetration depth up to 1–2 mm [5]. Two major types of OCT systems include time domain OCT (TD-OCT) and frequency or "Fourier" domain OCT (FD-OCT). FD-OCT is an advanced generation technology which offers improved signal-to-noise ratio and higher imaging speeds and diagnostic sensitivity compared to TD-OCT [7–9]. Long-range or "anatomic" OCT (LR-OCT) systems were later developed to allow for extended range imaging (axial range up to 25 mm) without sacrifice of resolution [10, 11].

Various OCT systems have been developed to allow for tissue scanning in a linear or radial fashion. Most in vivo OCT imaging of the OC or pharynx is accomplished using a fiber-optic probe which is placed in direct contact or near-contact with mucosal tissue. OCT sample arms may be housed in a rigid handheld instrument for intraoral or transoral imaging, integrated with the instrument channel of a flexible endoscope or applied to the pharynx in a flexible, transparent endoscopic catheter. Early TD-OCT systems had scan rates up to 1 kHz, axial resolution between 10 and 20 μm, and lateral resolution between 10 and 25 μm [12–17]. Later, swept source FD-OCT systems offered a substantial leap in scan rate (up to 100 kHz) and resolution (<10 μm) [18–22]. While the majority of OCT systems described in the literature are custom-built for research purposes, several TD-OCT and FD-OCT systems are available for commercial use including the United States Food and Drug Administration-approved Niris TD-OCT system (Imalux Corp., Cleveland, OH).

Diagnostic OCT of Mucosal Lesions

Animal and Ex Vivo Studies

In 2005, Wilder-Smith's group conducted in vivo OCT of oral premalignant and malignant lesions in hamster cheek pouch models [14]. OCT was combined with optical Doppler tomography (ODT) to image the epithelial and subepithelial layers of buccal mucosa as well as the structural integrity of the basement membrane. Several additional studies have reported OCT imaging epithelial and subepithelial structures with close correlation with histological samples in a hamster cheek pouch model [23–27].

In 2010, a group of researchers based at the University College London Hospital used a swept-source FD-OCT microscope (Michelson Diagnostics EX1301 OCT Microscope V1.0) to perform ex vivo OCT of suspicious oral lesions immediately following excisional or incisional biopsy [21]. Thirty-four oral lesions were analyzed for (1) architectural changes in keratin, epithelial, and

subepithelial layers, and identification of basement membrane, and (2) compared with histopathological results. While OCT data demonstrated distinct zones of normal and altered architectural changes, resolution was inadequate to identify exactly changes in pathologic tissue and, consequently, diagnosis and differentiation between dysplastic and malignant tissues was not possible. Additional reports of ex vivo OCT on human OC/OP tissues are included for review [28–31].

Clinical Studies

Select reports have focused solely on OCT imaging of normal, healthy mucosa of the OC/OP [12, 19, 32]. In 1998, Feldchtein et al. (Nizhny Novgorod, Russia) first reported in vivo OCT of hard and soft tissue of the oral cavity [12]. They used a dual wavelength TD-OCT system consisting of two superluminescent diodes operating at $\lambda_1 = 830$ nm and $\lambda_2 = 1280$ nm, respectively. Dual infrared beams with resolution of 17 μm (830 nm) and 22 μm (1280 nm) were aimed at masticatory, lining, and specialized oral mucosa to conduct transverse scanning. Single transverse scans were completed in 2–5 s, with simultaneous recording of OCT data from both signals. Differences in epithelial and lamina propria thickness were noted from different oral mucosa subtypes. The presence of keratin in the epithelium was also shown to reduce light penetration to underlying tissue layers, thus causing difficulty in distinguishing epithelium from lamina propria and submucosa in keratinized tissues. Later, Prestin et al. used OCT to measure epithelial thickness within the OC in 143 subjects [32]. Their data demonstrated varying epithelial thickness depending on location within the OC and provided a reference standard for differentiating normal from dysplastic tissue.

Numerous studies have evaluated in vivo OCT of benign or premalignant lesions of the OC and pharynx [15, 17, 20, 21, 33–35]. In 2006, Ridgway et al. imaged the OC and OP in 41 patients during operative endoscopy [15]. A TD-OCT system (central wavelength $\lambda = 1310$ nm, lateral and axial resolution ~10 μm) was used with a handheld fiber-optic probe (Fig. 4a) housed in a rigid, hollow metal tube (Fig. 4b). The probe was positioned manually or with endoscopic guidance and consisted of a gradient refractive index (GRIN) lens (1 mm diameter, 0.23 pitch) coupled with a right-angle prism to focus and reflect the OCT signal at 90. Their OCT data demonstrated normal microstructures, including keratinized epithelium, papillae, ducts, glands, and blood vessels, and benign pathologic features including mature scar, granulation tissue, mucous cysts, and leukoplakia.

A research team led by Betz and Kraft has been a forerunner in evaluating OCT in the diagnosis of lesions of the upper aerodigestive tract. Recently, they published multiple reports of in vivo imaging of OC anatomy and premalignant lesions using the Niris OCT imaging system (Imalux Corp.) [32, 35]. Their studies

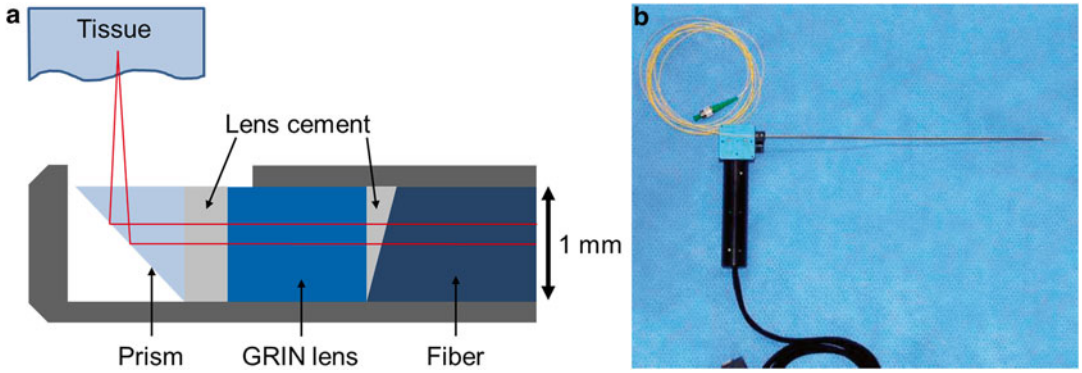

Fig. 4 Schematic of distal apparatus of endoscopic OCT probe (**a**) and rigid, hollow metal tubing for handheld, transoral application of OCT probe (**b**) constructed by Ridgway et al. [15]. *GRIN* gradient index refractive lens

reported that OCT-based differentiation between noninvasive and invasive lesions could be performed with 88.9 % sensitivity and 89.0 % specificity. Comparative analysis of OCT images from hyperplastic and dysplastic lesions demonstrated a statistically significant difference in intensity profiles of the epithelial layer between the two groups.

Other Oral Lesions and Dental Pathologies

Pharyngeal or oral mucositis (OM) is a toxic effect of chemotherapy and head and neck irradiation. At present, there is no means to predict the onset and severity of OM, thus limiting options for preventive and treatment measures. Early studies demonstrated OCT-based early detection and quantification of radiation- and chemotherapy-induced OM in mouse and hamster models [36, 37]. In 2007, Wilder-Smith et al. first reported OCT of chemotherapy-induced OM in human subjects [16]. Following commencement of chemotherapy, oral mucosa structure was longitudinally evaluated using a TD-OCT system (central wavelength $\lambda = 1310$ nm, axial resolution 10 μm) and a handheld fiber-optic probe. Their results demonstrated early and progressive changes in epithelial and subepithelial tissue thickness and integrity, prior to clinical manifestation of disease. The same group later reported TD-OCT of oral mucosa in 48 patients undergoing chemotherapy [38]. Using the Niris OCT system (Imalux Corp.), they demonstrated a higher sensitivity of detection for OM using OCT than using the gold standard OM assessment scale. Additional reports of OCT-based diagnosis of oral mucositis or postradiation changes are described in the literature [39–41]. Lee et al. performed swept-source OCT of healthy OC mucosa and oral submucosal fibrosis

and noted decreases in both epithelial thickness and standard deviation of A-mode scan intensity in mucosa with submucosal fibrosis compared to normal tissue [18].

There has been limited discussion on OCT of microvasculature and vascular malformations of the oral cavity [20, 22, 33, 37, 42]. In vivo assessment of microcirculation within OC tissues has potential to be a valuable diagnostic indicator due to the vascular change associated with pathologic lesions. Choi et al. conducted in vivo OCT of OC and nasal cavity microvasculature using a swept-source system (central wavelength $\lambda = 1300$ nm) coupled with a vertical cavity surface-emitting laser (VCSEL, coherence length ≥ 50 mm; Thorlabs, Inc. Newton, NJ, USA) [22]. A handheld probe (Thorlabs) was mounted in a positioning stage for oral and nasal cavity imaging. Side imaging (90° projection of OCT signal) and forward imaging (0° projection) scan modes were used to image circumferential or lateral wall tissues (e.g., buccal mucosa and nasal mucosa) and frontal regions (e.g., labial mucosa), respectively. Volumetric structural OCT images of oral and nasal cavity tissues were obtained to map blood perfusion. Additional studies have used ODT to detect functional blood flow within oral cavity tissue [37, 42]. ODT is a functional extension of OCT that measures phase change secondary to Doppler frequency shift of light backscattered from moving red blood cells within a blood vessel. Recently, speckle variance of OCT signal has been studied to analyze large blood vessels of the OC [33, 41].

Lastly, structural imaging of dental tissues has been evaluated using OCT. In 1997, Colston et al. first reported OCT of in vitro porcine periodontal tissues [43]. A transverse-scanning TD-OCT system (central wavelength $\lambda = 1310$ nm, resolution ~20 μm) coupled with a He–Ne laser (633 nm wavelength) was used to scan enamel–cementum and gingiva–tooth interfaces. OCT data were correlated with histological sections to demonstrate internal tooth and soft tissue structural relationships which are critical in the diagnosis of periodontal disease. Additional, early studies of TD-OCT imaging of dental structure are described [12, 44–46]. While this chapter does not cover OCT of dental structures, select articles on OCT applications in diagnostic evaluation and therapeutic monitoring in dentistry are included for review purposes [47–57].

Long-Range OCT

Upper airway obstruction is a frequently diagnosed condition among adult and pediatric patients and has potential for severe long-term sequela if untreated. A variety of pathologic conditions may be causative of upper airway obstruction including anatomic obstruction (e.g., deviated septum, stenosis, thickened palate, and collapse of aryepiglottic folds), tumors, tonsillar and/or adenoidal

hypertrophy, and congenital diseases (e.g., choanal atresia). Quantitative measurements of the pharyngeal lumen enable construction of virtual computational airway models to evaluate airflow. This information may help surgeons identify regions of airway stenosis, predict outcomes of medical or surgical intervention, and ultimately improve the management of OSA. At present, laryngoscopy and bronchoscopy remain the gold standard for diagnosis of upper airway obstructive disease, but only provide semiquantitative information on pharyngeal morphology. CT and MRI have been shown to provide quantitative upper airway dimensions; however, these techniques are associated with the need for sedation in children and ionizing radiation exposure (CT) and are limited by respiratory motion artifacts and long imaging times [58, 59].

LR-OCT or "anatomical" OCT is a minimally invasive endoscopic technique used to quantitatively assess the size and shape of the upper airway. Advantages of LR-OCT include high patient safety, portability, low cost, and long permissible patient exposure times given that OCT uses nonionizing radiation. In 2003, Armstrong et al. (Western Australia) first reported in vivo endoscopic LR-OCT of the upper airway in human subjects [10]. Using a frequency domain LR-OCT system (central wavelength $\lambda = 1325$ nm, axial resolution 17.4 μm), their group achieved long-range imaging (axial range 26 mm) using an endoscopic probe inserted through a transparent, distally sealed naso-esophageal catheter. The probe was rotated (3.75 Hz) to acquire stationary and continuous (0.2 mm/s pullback) cross-sectional images from the esophagus and pharynx. Further LR-OCT studies by the same group (Western Australia) demonstrated high correlation between LR-OCT and CT-derived measurements of pharyngeal cross-sectional area [60]. With the evolution of frequency domain technology, LR-OCT of the pharynx has been performed at helical scanning speeds up to 30 Hz [61] and axial imaging range up to 20 mm [11] in order to acquire three-dimensional volumetric images of the airway. LR-OCT images of select anatomic levels of the adult upper airway are depicted in Fig. 5. Additional reports of LR-OCT to quantitatively evaluate pharyngeal size and shape are described in the literature [11, 61–65].

OCT Limitations

The primary limitation of OCT is the optical penetration depth in biological tissue. Current OCT systems offer a maximum penetration depth of 1–2 mm. Achieving adequate signal penetration is imperative to differentiate between benign, premalignant, and malignant processes of the OC and pharynx. OCT diagnostic sensitivity is thus limited in the event of larger, exophytic lesions with high depths. Furthermore, OCT signal absorption and/or

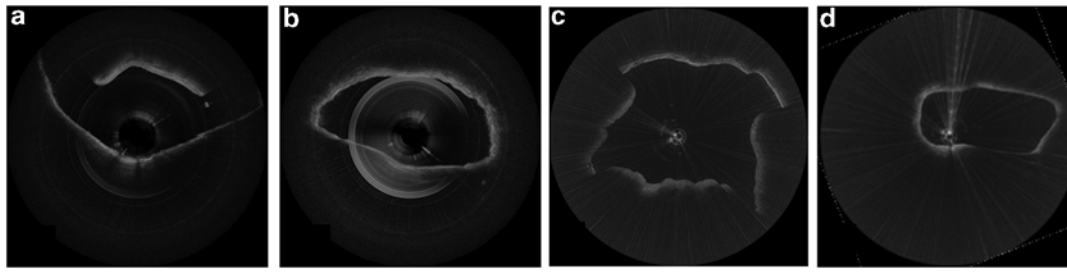

Fig. 5 Long-range OCT images of the tip of epiglottis (**a**), base of tongue (**b**), adenoids (**c**), and choana (**d**) from an adult upper airway. All OCT images are displayed in polar coordinates, with anterior tissues at the top of the image

scattering by tissues such as cartilage and bone results in distal shadows on cross-sectional images and further limits the diagnostic sensitivity in mixed hard–soft tissues. Additional factors which may limit image quality for in vivo imaging include physician hand tremor, patient movement, and equipment vibrations; such movements translate to reverberating effects on measured optical backscattering and can result in image distortion or stretching. Lastly, although advanced FD-OCT systems offer a peak resolution of approximately 10 μm, this precludes tissue diagnosis at the cellular level. Hence, OCT cannot provide definitive differentiation between premalignant and malignant lesions, necessitating histologic analysis of excised tissue.

Malignancy

In 2014, an estimated 42,440 new cases of oral cavity and pharyngeal cancer will be diagnosed in the United States [66]. A majority of these cancers are squamous cell carcinomas, which are preceded by dysplastic lesions including white (leukoplakia), red (erythroplakia), or mixed epithelial lesions. These lesions may progress to cancer, with erythroplakia (51 %) lesions more likely to undergo malignant transformation than leukoplakia (5 %) [2, 3]. Fundamental to long-term survival is early diagnosis and routine follow-up with the otolaryngologist for close monitoring of disease. Optical diagnostics holds promise for minimally invasive, cost-effective, and early detection of malignant lesions in the head and neck. While OCT resolution limits preclude the definitive diagnosis of malignant lesions, OCT may be used as an adjunct imaging modality to guide biopsy decisions and localize subclinical disease. A thorough review of OCT research in the diagnosis of malignant lesions in the upper aerodigestive tract is described elsewhere in this text.

References

1. Lian T. Benign tumors and tumor-like lesions of the oral cavity. In: Robbins K, Haughey B, editors. Cummings otolaryngology head & neck surgery. Philadelphia, PA: Mosby Elsevier; 2010. p. 1287–93.
2. Reibel J. Prognosis of oral pre-malignant lesions: significance of clinical, histopathological, and molecular biological characteristics. Crit Rev Oral Biol Med. 2003;14(1):47–62.
3. Walsh T, et al. Clinical assessment to screen for the detection of oral cavity cancer and potentially malignant disorders in apparently healthy adults. Cochrane Database Syst Rev. 2013;11:CD010173.
4. Tan L, Loh T. Benign and malignant tumors of the nasopharynx. In: Robbins K, Haughey B, editors. Cummings otolaryngology head & neck surgery. Philadelphia, PA: Mosby Elsevier; 2010. p. 1348–58.
5. Huang D, et al. Optical coherence tomography. Science. 1991;254(5035):1178–81.
6. Fercher AF. Optical coherence tomography—development, principles, applications. Z Med Phys. 2010;20(4):251–76.
7. Beaurepaire E, et al. Full-field optical coherence microscopy. Opt Lett. 1998;23(4):244–6.
8. Choma M, et al. Sensitivity advantage of swept source and Fourier domain optical coherence tomography. Opt Express. 2003;11(18):2183–9.
9. Yun S, et al. High-speed optical frequency-domain imaging. Opt Express. 2003;11(22):2953–63.
10. Armstrong J, et al. In vivo size and shape measurement of the human upper airway using endoscopic longrange optical coherence tomography. Opt Express. 2003;11(15):1817–26.
11. Jing J, et al. High-speed upper-airway imaging using full-range optical coherence tomography. J Biomed Opt. 2012;17(11):110507.
12. Feldchtein F, et al. In vivo OCT imaging of hard and soft tissue of the oral cavity. Opt Express. 1998;3(6):239–50.
13. Feldchtein F, et al. Endoscopic applications of optical coherence tomography. Opt Express. 1998;3(6):257–70.
14. Wilder-Smith P, et al. Noninvasive imaging of oral premalignancy and malignancy. J Biomed Opt. 2005;10(5):051601.
15. Ridgway JM, et al. In vivo optical coherence tomography of the human oral cavity and oropharynx. Arch Otolaryngol Head Neck Surg. 2006;132(10):1074–81.
16. Kawakami-Wong H, et al. In vivo optical coherence tomography-based scoring of oral mucositis in human subjects: a pilot study. J Biomed Opt. 2007;12(5):051702.
17. Wilder-Smith P, et al. In vivo diagnosis of oral dysplasia and malignancy using optical coherence tomography: preliminary studies in 50 patients. Lasers Surg Med. 2009;41(5):353–7.
18. Lee CK, et al. Diagnosis of oral submucous fibrosis with optical coherence tomography. J Biomed Opt. 2009;14(5):054008.
19. Ozawa N, et al. In vivo imaging of human labial glands using advanced optical coherence tomography. Oral Surg Oral Med Oral Pathol Oral Radiol Endod. 2009;108(3):425–9.
20. Ozawa N, et al. Evaluation of oral vascular anomalies using optical coherence tomography. Br J Oral Maxillofac Surg. 2009;47(8):622–6.
21. Jerjes W, et al. In vitro examination of suspicious oral lesions using optical coherence tomography. Br J Oral Maxillofac Surg. 2010;48(1):18–25.
22. Choi WJ, Wang RK. In vivo imaging of functional microvasculature within tissue beds of oral and nasal cavities by swept-source optical coherence tomography with a forward/side-viewing probe. Biomed Opt Express. 2014;5(8):2620–34.
23. Dong H, et al. Quantitative analysis on tongue inspection in traditional Chinese medicine using optical coherence tomography. J Biomed Opt. 2008;13(1):011004.
24. Graf RN, Brown WJ, Wax A. Parallel frequency-domain optical coherence tomography scatter-mode imaging of the hamster cheek pouch using a thermal light source. Opt Lett. 2008;33(12):1285–7.
25. Graf RN, et al. Detecting precancerous lesions in the hamster cheek pouch using spectroscopic white-light optical coherence tomography to assess nuclear morphology via spectral oscillations. J Biomed Opt. 2009;14(6):064030.
26. Hammer-Wilson MJ, et al. Detection of vesicant-induced upper airway mucosa damage in the hamster cheek pouch model using optical coherence tomography. J Biomed Opt. 2010;15(1):016017.
27. Park J, et al. A dual-modality optical coherence tomography and fluorescence lifetime imaging microscopy system for simultaneous morphological and biochemical tissue characterization. Biomed Opt Express. 2010;1(1):186–200.

28. Hamdoon Z, et al. Structural validation of oral mucosal tissue using optical coherence tomography. Head Neck Oncol. 2012;4:29.
29. Adegun OK, et al. Quantitative analysis of optical coherence tomography and histopathology images of normal and dysplastic oral mucosal tissues. Lasers Med Sci. 2012;27(4):795–804.
30. Adegun OK, et al. Quantitative optical coherence tomography of fluid-filled oral mucosal lesions. Lasers Med Sci. 2013;28(5):1249–55.
31. Hamdoon Z, et al. Optical coherence tomography in the assessment of suspicious oral lesions: an immediate ex vivo study. Photodiagn Photodyn Ther. 2013;10(1):17–27.
32. Prestin S, et al. Measurement of epithelial thickness within the oral cavity using optical coherence tomography. Head Neck. 2012;34(12):1777–81.
33. Davoudi B, et al. Noninvasive in vivo structural and vascular imaging of human oral tissues with spectral domain optical coherence tomography. Biomed Opt Express. 2012;3(5):826–39.
34. Lee CK, et al. Diagnosis of oral precancer with optical coherence tomography. Biomed Opt Express. 2012;3(7):1632–46.
35. Volgger V, et al. Evaluation of optical coherence tomography to discriminate lesions of the upper aerodigestive tract. Head Neck. 2013;35(11):1558–66.
36. Muanza TM, et al. Evaluation of radiation-induced oral mucositis by optical coherence tomography. Clin Cancer Res. 2005;11(14):5121–7.
37. Wilder-Smith P, et al. In vivo imaging of oral mucositis in an animal model using optical coherence tomography and optical Doppler tomography. Clin Cancer Res. 2007;13(8):2449–54.
38. Calantog A, et al. A prospective study to assess in vivo optical coherence tomography imaging for early detection of chemotherapy-induced oral mucositis. Lasers Surg Med. 2013;45(1):22–7.
39. Gladkova ND, et al. Potential of optical coherence tomography for diagnosing mucositis in cancer of the nasal cavity and throat in the course of radio- and chemoradiotherapy. Vopr Onkol. 2006;52(4):443–7.
40. Maslennikova AV, et al. Use of optical coherence tomography for prognosis of the severity of oral mucositis. Vopr Onkol. 2009;55(5):572–9.
41. Davoudi B, et al. Optical coherence tomography platform for microvascular imaging and quantification: initial experience in late oral radiation toxicity patients. J Biomed Opt. 2013;18(7):76008.
42. Otis LL, et al. Quantifying labial blood flow using optical Doppler tomography. Oral Surg Oral Med Oral Pathol Oral Radiol Endod. 2004;98(2):189–94.
43. Colston BW, et al. Optical coherence tomography for diagnosing periodontal disease. Proc SPIE. 1997;2973:216–20. Lasers in Dentistry III.
44. Colston Jr BW, et al. Imaging of hard- and soft-tissue structure in the oral cavity by optical coherence tomography. Appl Opt. 1998;37(16):3582–5.
45. Warren JA, et al. Imaging and characterization of dental structure using optical coherence tomography. Opt Soc Am: Tech Dig Ser. 1998;6:128.
46. Baek JH, et al. Optical approach to the salivary pellicle. J Biomed Opt. 2009;14(4):044001.
47. Baumgartner A, et al. Polarization-sensitive optical coherence tomography of dental structures. Caries Res. 2000;34(1):59–69.
48. Fried D, et al. Imaging caries lesions and lesion progression with polarization sensitive optical coherence tomography. J Biomed Opt. 2002;7(4):618–27.
49. Chen Y, et al. Characterization of dentin, enamel, and carious lesions by a polarization-sensitive optical coherence tomography system. Appl Opt. 2005;44(11):2041–8.
50. de Melo LS, et al. Evaluation of enamel dental restoration interface by optical coherence tomography. J Biomed Opt. 2005;10(6):064027.
51. Gimbel C. Optical coherence tomography diagnostic imaging. Gen Dent. 2008;56(7):750–7. Quiz 758–9, 768.
52. Kang H et al. Imaging early demineralization with PS-OCT. Proc SPIE Int Soc Opt Eng. 2010;7549. http://www.ncbi.nlm.nih.gov/pubmed/22399835
53. Park KJ, Schneider H, Haak R. Assessment of interfacial defects at composite restorations by swept source optical coherence tomography. J Biomed Opt. 2013;18(7):076018.
54. Chan KH, et al. A method for monitoring enamel erosion using laser irradiated surfaces and optical coherence tomography. Lasers Surg Med. 2014;46(9):672–8.
55. Nee A, et al. Longitudinal monitoring of demineralization peripheral to orthodontic brackets using cross polarization optical coherence tomography. J Dent. 2014;42(5):547–55.
56. Nakajima Y, et al. Detection of occlusal caries in primary teeth using swept source optical coherence tomography. J Biomed Opt. 2014;19(1):16020.

57. Marcauteanu C, et al. Quantitative evaluation of dental abfraction and attrition using a swept-source optical coherence tomography system. J Biomed Opt. 2014;19(2):21108.
58. Arens R, et al. Linear dimensions of the upper airway structure during development: assessment by magnetic resonance imaging. Am J Respir Crit Care Med. 2002;165(1):117–22.
59. Abramson Z, et al. Age-related changes of the upper airway assessed by 3-dimensional computed tomography. J Craniofac Surg. 2009;20 Suppl 1:657–63.
60. Armstrong JJ, et al. Quantitative upper airway imaging with anatomic optical coherence tomography. Am J Respir Crit Care Med. 2006;173(2):226–33.
61. Wijesundara K, et al. Quantitative upper airway endoscopy with swept-source anatomical optical coherence tomography. Biomed Opt Express. 2014;5(3):788–99.
62. Leigh MS, et al. Anatomical optical coherence tomography for long-term, portable, quantitative endoscopy. IEEE Trans Biomed Eng. 2008;55(4):1438–46.
63. Walsh JH, et al. Evaluation of pharyngeal shape and size using anatomical optical coherence tomography in individuals with and without obstructive sleep apnoea. J Sleep Res. 2008;17(2):230–8.
64. Walsh JH, et al. Effect of body posture on pharyngeal shape and size in adults with and without obstructive sleep apnea. Sleep. 2008; 31(11):1543–9.
65. Cisonni J, et al. Effect of the velopharynx on intraluminal pressures in reconstructed pharynges derived from individuals with and without sleep apnea. J Biomech. 2013;46(14): 2504–12.
66. Society AC. Cancer facts & figures 2014. Atlanta: American Cancer Society; 2014.